

CHAPTER 8: BREAST STRAIN IMAGING: A CAD FRAMEWORK

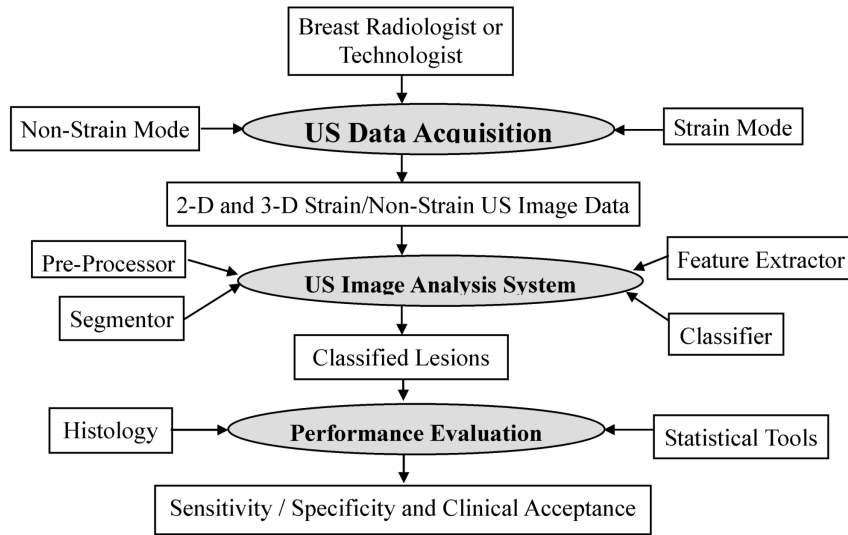
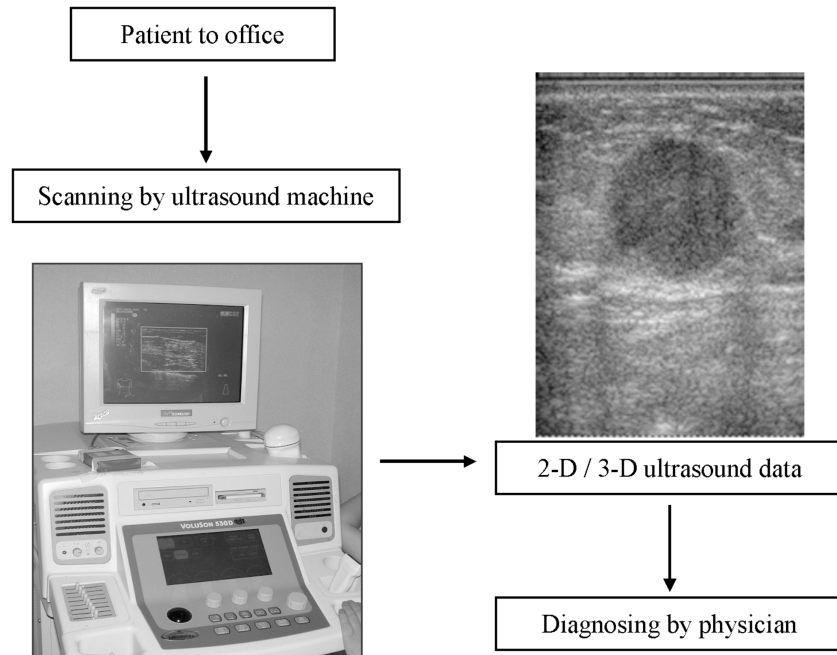


Figure 1. General ultrasound image analysis architecture.



* Photograph source: Voluson 530 (Kretz Technik, Austria) scanner.

Figure 2. Typical automatic image acquisition system. Photographic source: Voluson 530 (Kretz Technik, Austria) scanner.

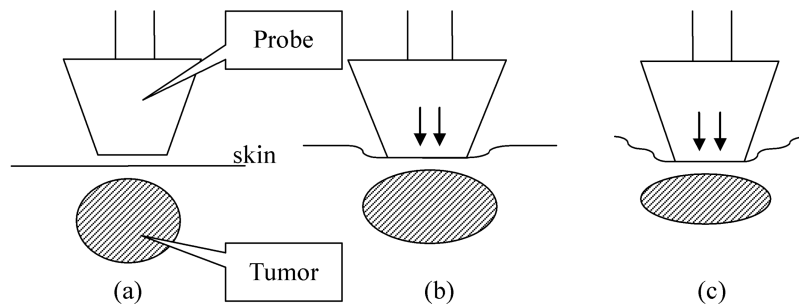


Figure 3. (a) Pre-compression; (b) post-compression (intermediate stage), and (c) post-compression (final stage).

CHAPTER 8: BREAST STRAIN IMAGING: A CAD FRAMEWORK

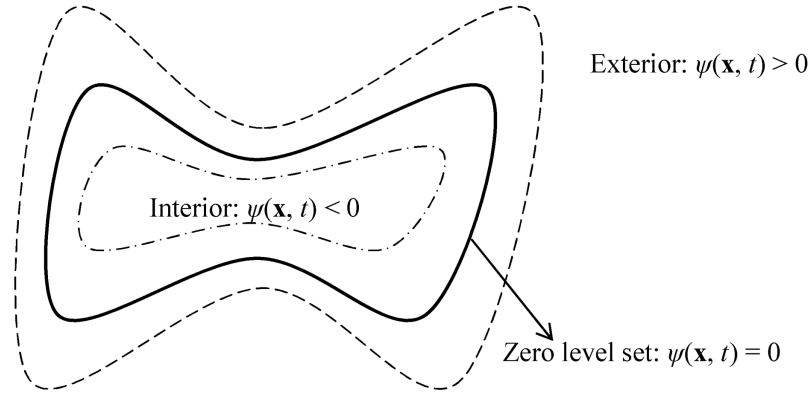


Figure 4. The sign of $\psi(x, t)$ is decided by whether the point is in the interior (minus) or exterior (plus) of the zero level set.

				2.5	1.9	2.7			
		1.8	1.5	1.3	0.2	0.8	1.9		
	2.1	0.8	0.4	-0.3	-1.1	0.1	0.9	2.2	
2.6	1.1	0.1	-0.8	-1.3	-2.3	-1.6	0	1.1	3.0
1.8	0.1	-1.2	-2.2	-3.1	-4.8	-3.6	-0.9	-0.1	1.8
2.1	-0.3	-0.2	-0.7	-1.6	-2.6	-2.9	-0.8	0.4	2.2
2.9	1.6	0.1	0.2	0	-1.5	-1.0	0	1.4	3.2
	2.3	0.9	1.0	0.1	-0.9	-0.5	0.3	1.2	
			1.8	0.7	-0.3	0.2	0.8	2.8	
				1.9	1.4	1.1	2.5		

Figure 5. Implicit level set surface ψ is the dotted line superimposed over the image grid. The location of the surface is interpolated by the image pixel values. The grid pixels closest to the implicit surface are shown in gray.

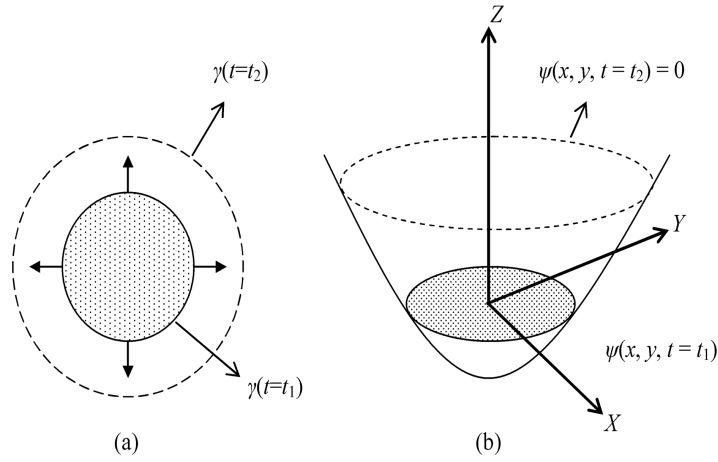


Figure 6. Level set formulation of equations of motion: (a) arrows show the propagating direction of the front $\gamma(t = t_1)$; (b) the corresponding surface $\psi(x, y)$ at time t_2 .

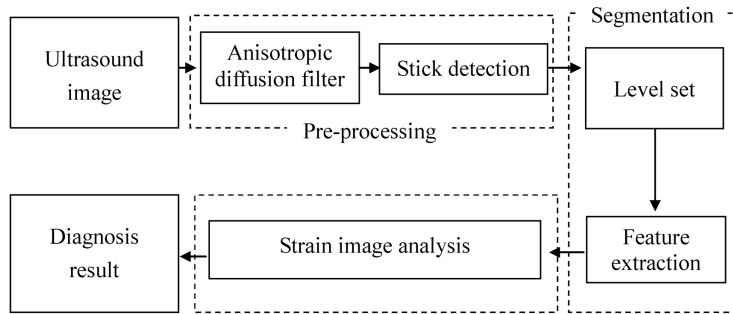


Figure 7. 2D breast lesion characterization system.

CHAPTER 8: BREAST STRAIN IMAGING: A CAD FRAMEWORK

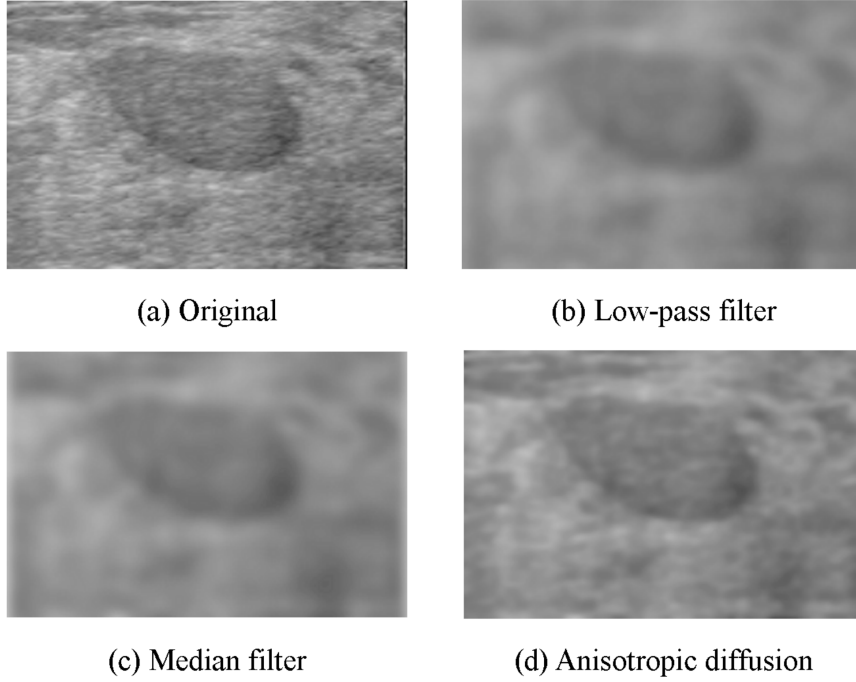


Figure 8. A blurring example with different filters: (a) original benign tumorw; (b) using a low-pass filter; (c) median filter; (d) anisotropic diffusion filter.

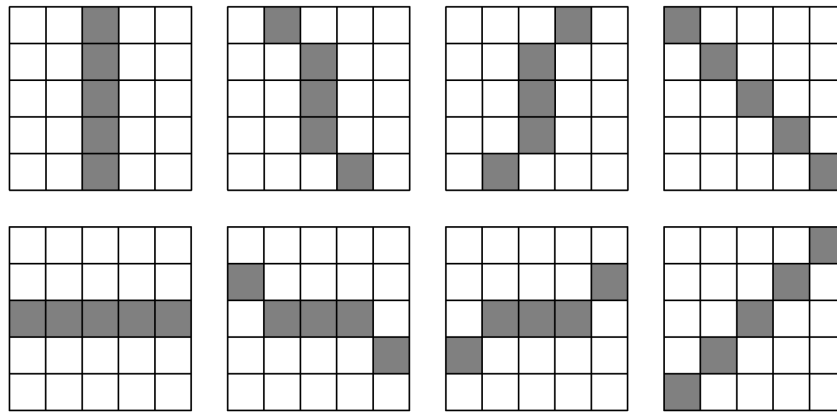


Figure 9. Eight possible orientations of a stick with a length of five (5×5 masks).

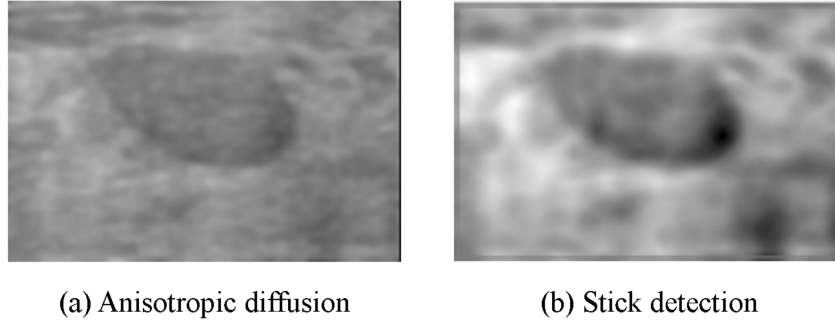


Figure 10. (a) The same example as in Figure 8d; (b) after applying stick detection using 5×5 masks.

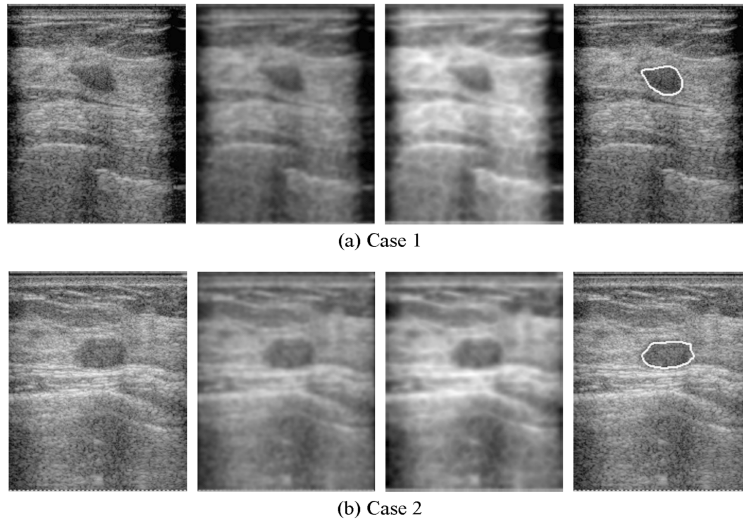


Figure 11. Two segmentation results for benign tumor cases using the level set method. For each case, the first image is the original one, the second was processed using an anisotropic diffusion filter, the third was enhanced using stick detection and the final one was processed using the level set method.

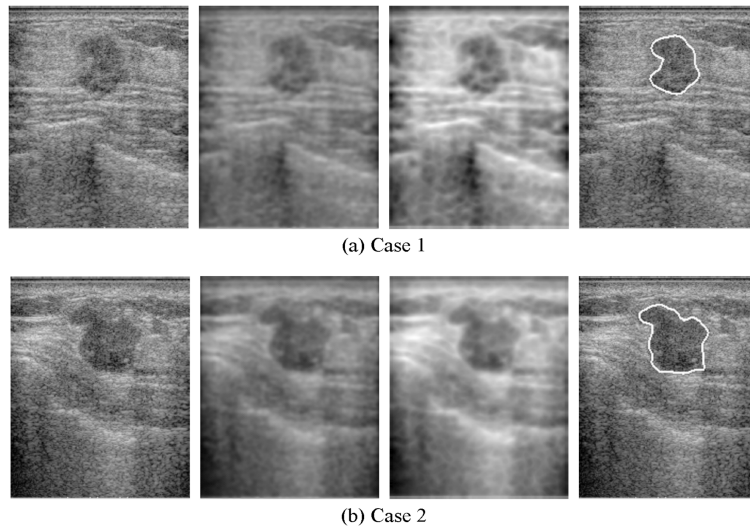


Figure 12. Two segmentation results for malignant tumor cases using the level set method. For each case, the first image is the original one, the second was processed using an anisotropic diffusion filter, the third was enhanced using stick detection and the final one was processed using the level set method.

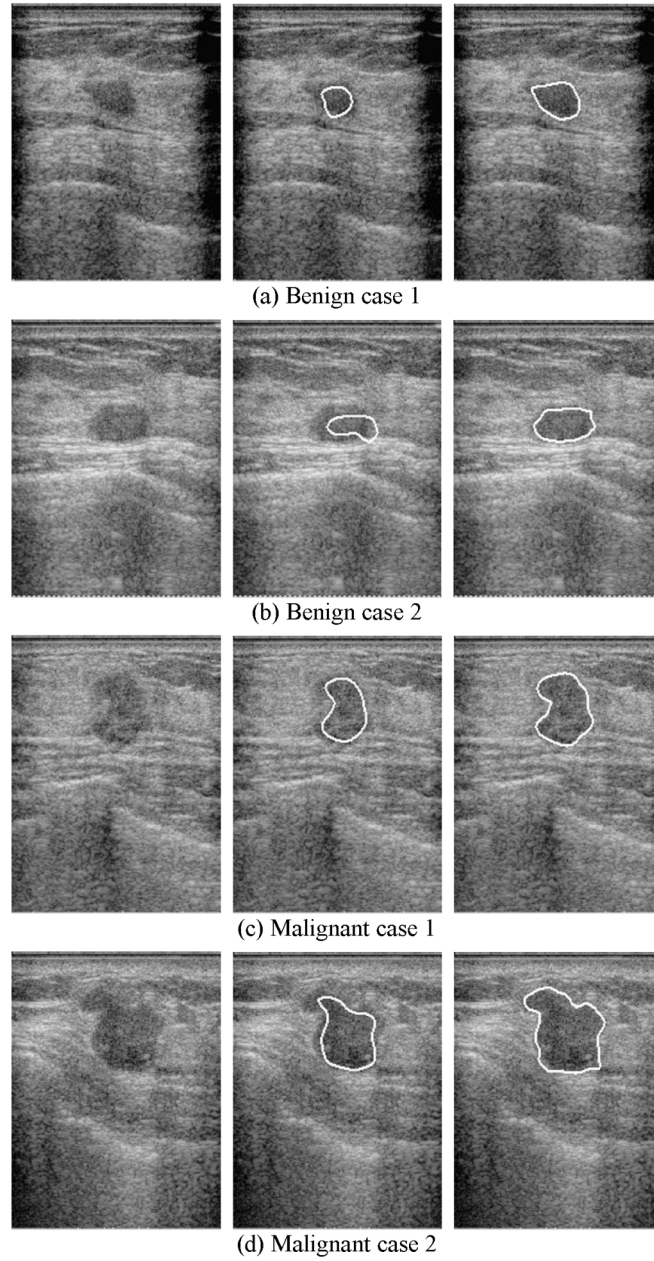


Figure 13. Result of using the level set method on non-enhanced and enhanced images. For each case, the first is the original image, the middle one was processed using the level set method, and the final image was based on image preprocessing, as in Figures 11 and 12.

CHAPTER 8: BREAST STRAIN IMAGING: A CAD FRAMEWORK

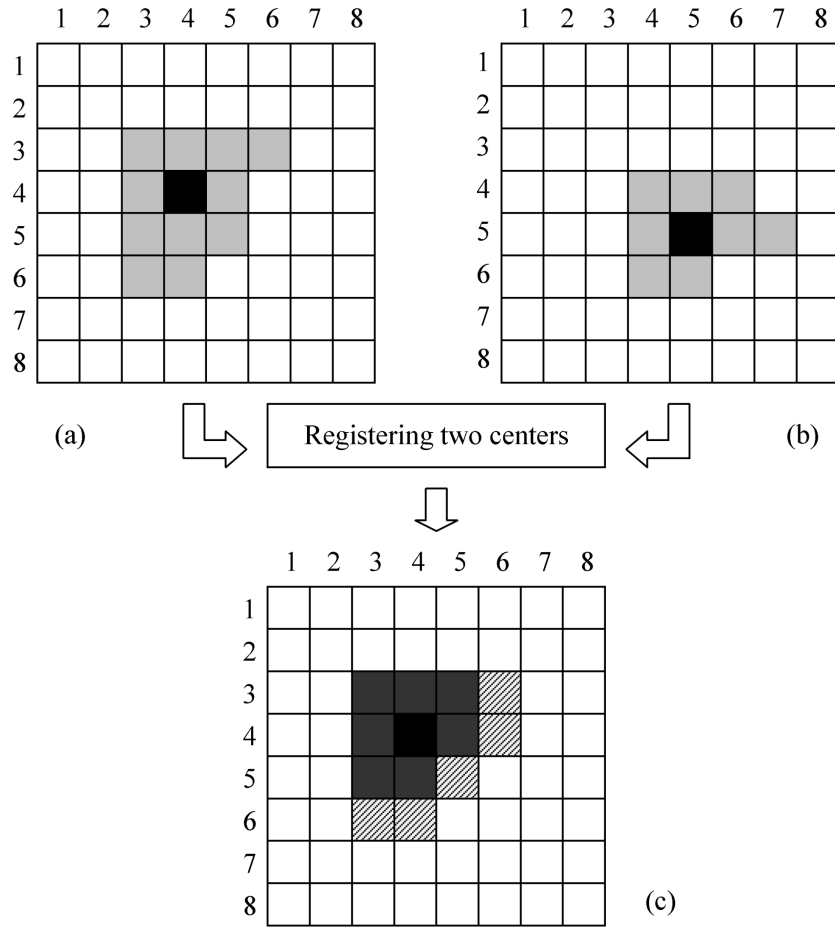


Figure 14. An example of computing C_d : (a) reference image; (b) moving image; (c) after registering (b) to (a) the contour difference is obtained.

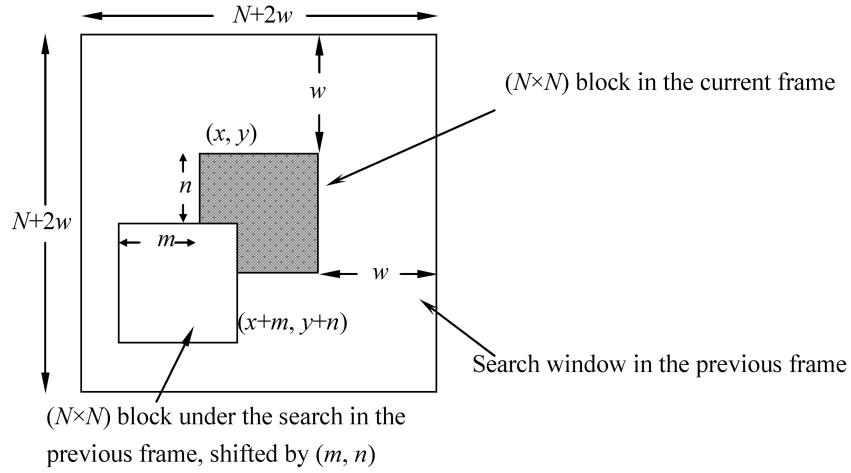


Figure 15. An example of computing shift distance.

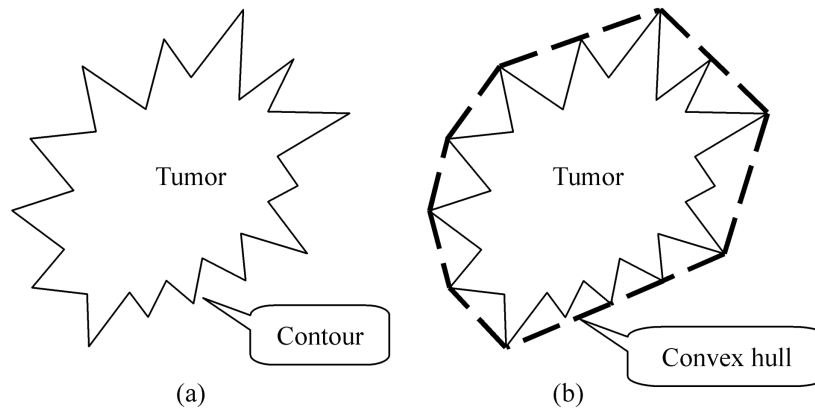


Figure 16. Drawings depict (a) the contour of a tumor, and (b) the convex hull of a tumor. The outer polygon (arrow) is the convex hull of the tumor, while the convex hull is the smallest convex set containing the tumor.

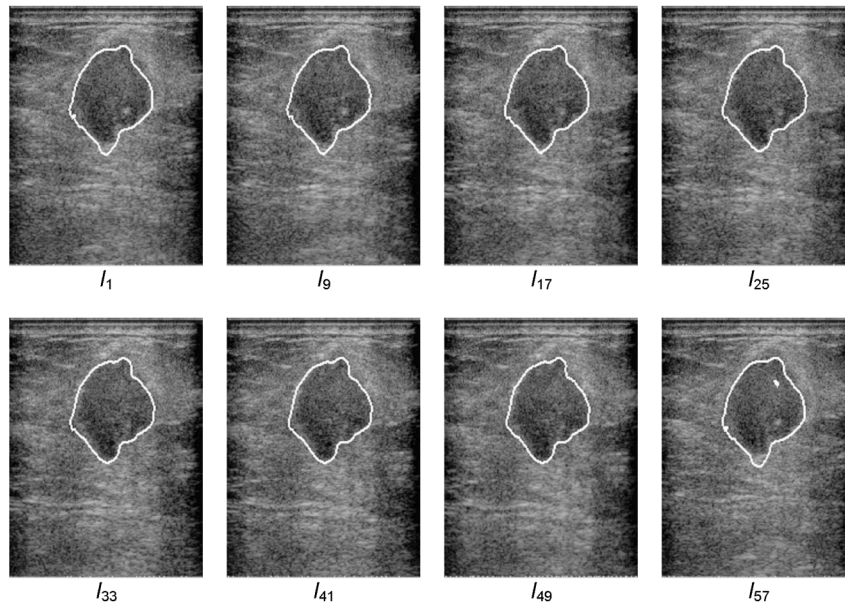


Figure 17. The first segmentation results for the malignant case in different image slices with $C_d = 1.18\%$, $M_d = 1.196$, $A_d = 0.33\%$, and $S_o = 0.8734$.

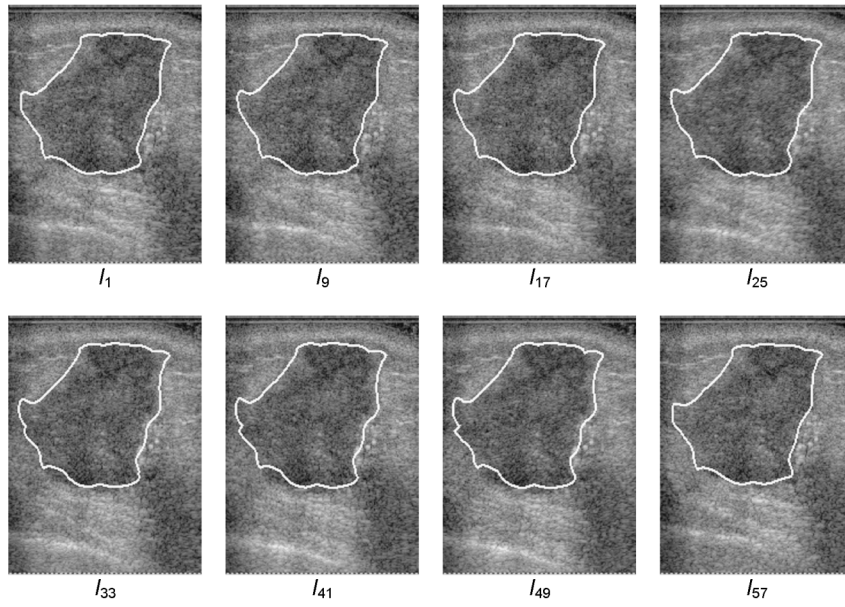


Figure 18. The second segmentation results for the malignant case in different image slices with $C_d = 1.20\%$, $M_d = 1.241$, $A_d = 0.85\%$, and $S_o = 3.6919$.

CHAPTER 8: BREAST STRAIN IMAGING: A CAD FRAMEWORK

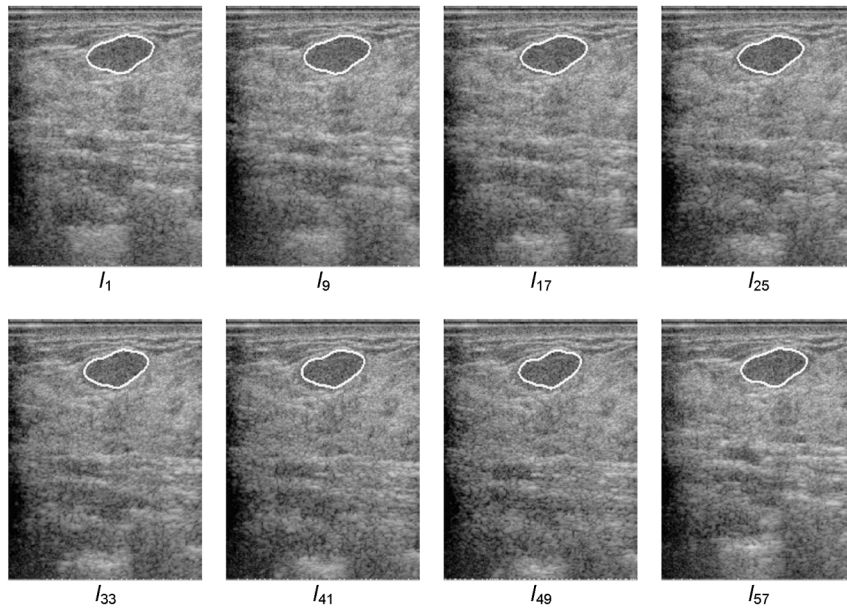


Figure 19. The first segmentation results for the benign case in different image slices with $C_d = 16.90\%$, $M_d = 7.161\%$, $A_d = 1.71\%$, and $S_o = 0.1876$.

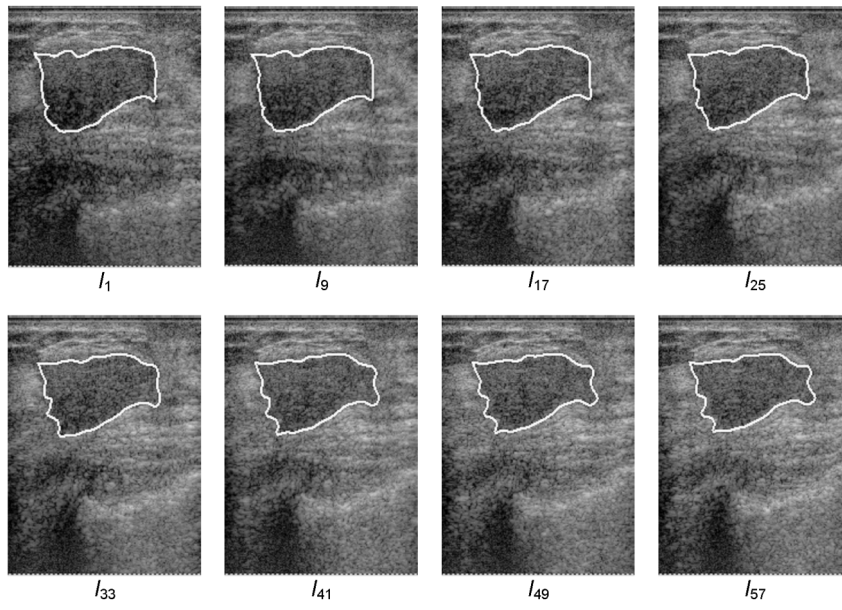


Figure 20. The second segmentation results for the benign case in different image slices with $C_d = 4.73\%$, $M_d = 1.90\%$, $A_d = 1.78\%$, and $S_o = 1.86$.

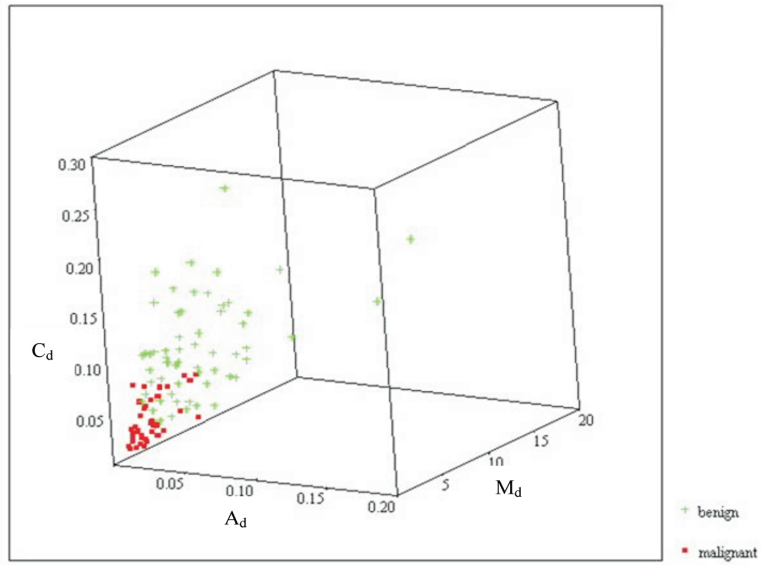


Figure 21. Scatter graph showing contour difference (C_d), area difference (A_d), and shift distance (M_d) of all the benign and malignant breast tumors.

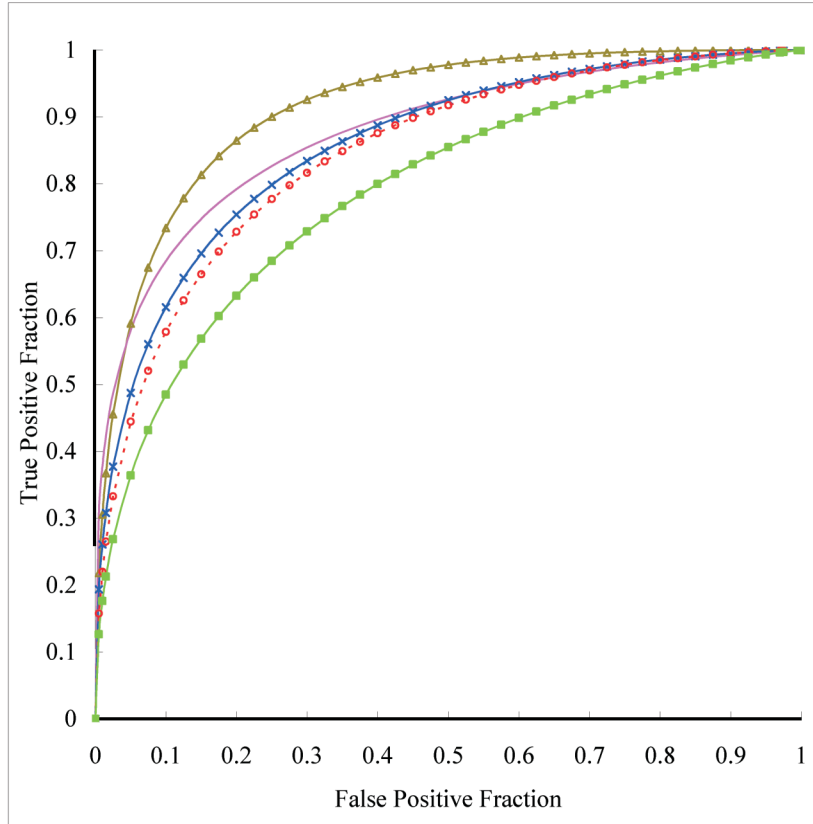


Figure 22. ROC analysis of all 2D strain features. Note that C_d is contour difference, A_d is area difference, M_d is shift distance, S_o is the solidity value, and A_z is the area under the curve. The SVM using all four features produced the best performance, with an A_z value of 0.91.